Effect of Retained Austenite Stabilized *via* Quench and Partitioning on the Strain Hardening of Martensitic Steels

E. DE MOOR, S. LACROIX, A.J. CLARKE, J. PENNING, and J.G. SPEER

A novel heat-treating process, quench and partitioning (Q&P), has been proposed as a fundamentally new way to produce martensitic microstructures containing retained austenite. The two-step process hypothesizes carbon enrichment of the austenite by decarburization of the martensite. Significant amounts of retained austenite have been measured in the final microstructure, although evidence for transition carbide formation in the martensite also exists. The mechanical properties obtained *via* Q&P are reported for a CMnAlSiP steel after intercritical annealing for A50 specimens. Tensile strength/total elongation combinations, ranging from 800 MPa/ > 25 pct to 900 MPa/20 pct to 1000 MPa/10 pct, indicate that Q&P is a viable way to produce high strength steel grades with good ductility. The instantaneous strain hardening of Q&P steels shows a significant dependence on the partitioning conditions applied. Lower partitioning temperature (PT) leads to continuously decreasing instantaneous *n*-values with strain, similar to the strain hardening behavior observed for dual-phase (DP) steels, whereas higher PTs for the same partitioning time increase the strain hardening significantly. After an initial increase, the observed *n*-values remain high up to considerable amounts of strain, resulting in similar strain hardening behavior observed for austempered transformation-induced plasticity (TRIP) grades. Assessment of the mechanical stability of the retained austenite indicates that the TRIP effect is effectively contributing to the increased strain hardening as function of strain.

DOI: 10.1007/s11661-008-9609-z

I. INTRODUCTION

INCREASED passenger car safety regulations and environmental concerns have led to the development and increased use of several types of advanced high strength steel grades (AHSS). The primary goal of the development of AHSS has usually been an increase of strength without significant formability loss, allowing for the production and application of thinner gaged, high strength automotive body parts. The resulting decrease in car body weight leads to reduced fuel consumption and emissions. Dual-phase (DP) and transformation-induced plasticity (TRIP) steel grades are two such types of AHSS used for automotive applications. Due to their multiphase nature, a composite effect between a hard, high strength martensitic or bainitic constituent and a soft, ductile ferritic phase results in high strength and good ductility. Metastable carbon-rich austenite in TRIP steels is retained during the bainitic transformation upon isothermal holding (austempering). Carbon is rejected from the bainitic ferrite into the surrounding austenite, thereby reducing its M_s temperature and promoting stability at room temperature. In TRIP steels, the onset of necking is postponed by the strain-induced transformation of the metastable austenite to hard martensite. This transformation is accompanied by a volume expansion and dislocations are introduced to accommodate the misfit between the austenite and martensite. The transformation of the metastable austenite thus leads to increased strain hardening, a characteristic often typical of TRIP steels. Quench and partitioning (Q&P) stabilizes austenite in a martensitic microstructure and may also lead to increased strain hardening in these high strength microstructures if the TRIP effect is operating.

II. QUENCH AND PARTITIONING

A thermal processing route, Q&P, was proposed by Speer *et al.*[1] as a new concept to produce martensitic microstructures containing enhanced levels of retained austenite. The process consists of a two-step heat treatment. After reheating in order to obtain a fully austenitic or intercritical microstructure, the steel is quenched to a suitable predetermined temperature in the M_s-M_f region. The desired microstructure at this quench temperature (QT) consists of martensite (α_M) and untransformed austenite. In a second step, the steel is either held at the QT or brought to a higher temperature, the so-called partitioning temperature (PT). The

E. DE MOOR, Graduate Student, and J. PENNING, Professor, are with Laboratory for Iron and SteelMaking (lism), Department of Metallurgy and Materials Science, Ghent University, B-9052 Zwijnaarde, Belgium. Contact e-mail: emmanuel.demoor@ugent.be S. LACROIX, Research Engineer, is with Arcelor-Mittal Research Industry Ghent OCAS NV Arcelor-Mittal Group, B-9060 Zelzate, Belgium. A.J. CLARKE, Postdoctoral Research Associate, is with Materials Science and Technology Division, Los Alamos National Laboratory, Los Alamos, NM 87545. J.G. SPEER, Professor, is with Advanced Steel Processing and Products Research Center, Colorado School of Mines, Golden, CO 80401.

Manuscript submitted September 30, 2007.
Article published online July 30, 2008

aim of the latter step is to carbon-enrich the untransformed austenite remaining at the QT through carbon depletion of the carbon supersaturated martensite. Through this concept, a martensitic microstructure along with metastable retained austenite is intended to be present after final quenching.

For the greatest austenite fractions to be retained in the Q&P process, formation of carbides (either transition carbide or cementite) should be avoided as much as possible, because carbides act as carbon "sinks" and therefore reduce the capacity for partitioning of carbon into austenite. Cementite formation can be effectively suppressed by alloying with Si, Al, or P.[2–4] These elements are considered insoluble in cementite, and growth of cementite is considered to require rejection of Si, Al, or P. Silicon is also known to deteriorate galvanizability due to the formation of oxides adherent to the steel substrate.[5] Partial replacement of Si by Al or P has been shown to effectively retard cementite formation without a detrimental effect on hot-dip coatability in TRIP steels.[6] Unlike the effect on cementite formation, the effect of Si, Al, and P on transition carbide formation is less clear. It is believed that these carbides are able to incorporate the elements as solutes, and that alloying with these elements does not effectively suppress transition carbide formation. The ε or η transition carbides are known to precipitate readily in the early stages of martensite tempering or upon quenching (so-called autotempering).[7–9] Such dispersions of transition carbides have also been observed after Q&P processing of a 0.6 wt pct carbon Si-containing steel,[10,11] especially at low PTs.[12] In lower carbon sheet steels processed by Q&P, some transition carbides were also observed[12–14] although the number densities of these carbides usually appeared rather low, and the extent of carbide formation is again believed to be dependent on partitioning conditions.[12,13,15]

Another aspect that should be considered during Q&P processing is the stability of the austenite during holding at the QT and during subsequent partitioning (usually at a higher temperature). If bainite formation or migration of the austenite/martensite interface are able to occur during partitioning, then austenite present at the QT may be consumed, reducing the capacity for austenite stabilization through the proposed partitioning mechanism. While further studies of interface migration during partitioning are needed,[16,17] a recent analysis by Clarke *et al*. suggested that measured retained austenite volume fractions and associated carbon concentrations in a Si-Mn sheet steel processed by Q&P could not be attributed solely to the formation of bainitic ferrite and associated carbon rejection.[18] While these fundamental details related to microstructural evolution are not central to the mechanical behaviors reported here, they are relevant to interpretation of the results and understanding/optimization of the Q&P process.

In the present contribution, a 0.17C-1.65Mn-0.38Si-1.11Al-0.08P (wt pct) steel is Q&P heat treated and the mechanical properties are assessed. A comparison is made with TRIP and quenched and tempered (Q&T) DP microstructures produced in the same alloy, to assess the potential benefits of the Q&P microstructure. Because retained austenite is present in combination with a martensitic microstructure in Q&P processing, it is hypothesized that higher strength levels may be obtained compared to TRIP steels, while the presence of retained austenite may provide increased ductility compared to DP microstructures. The mechanical stability of the retained austenite is measured and compared with the stability of the austenite retained after a bainitic transformation.

III. EXPERIMENTAL PROCEDURE

Commercially produced, cold rolled 0.17C-1.65Mn-0.38Si-1.11Al-0.08P (wt pct) sheet steel was received in the full hard condition. Tensile specimens were machined in the rolling direction according to the A50 geometry shown in Figure 1. Annealing was done using salt baths according to the scheme given in Figure 2. The annealing parameters selected are compatible with modern annealing line capabilities.[19] Initial reheating was done at 850 °C for 150 seconds. Approximately 64 vol pct intercritical ferrite (α_{int}) was present at this temperature based on dilatometry measurements, whereas 47 vol pct was predicted by ThermoCalc. An M_s temperature of 357 °C was measured after intercritical annealing, in good agreement with the formula proposed by Mahieu.[20] The QT effects were calculated using a model that incorporates the assumption of full carbon depletion of the martensite during partitioning.[1] The results are shown in Figure 3. It should be recognized that the assumption of full carbon depletion of martensite represents an idealized partitioning condition that provides an "upper bound" to the calculations, which is useful for process design. This assumption is not considered to be strictly applicable under generalized conditions in real steels where competing processes may occur, such as transition carbide or cementite formation, austenite decomposition, dislocation trapping, *etc*. as mentioned previously. Preliminary heat treatments were conducted to assess experimentally the influence of QT variations on final austenite fraction, under fixed partitioning conditions involving 120 seconds at 400 °C (data included in Figure 3). In comparison to the model calculations, the measured austenite fractions were less sensitive to QT variations,

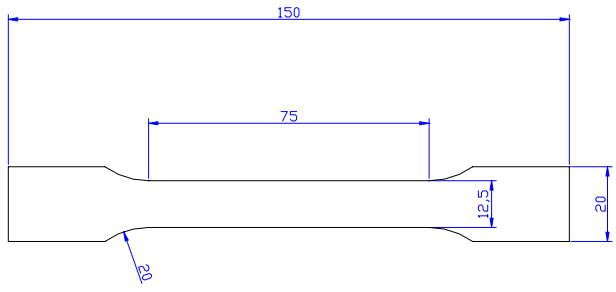

Fig. 1—Geometry of A50 tensile test specimen. All dimensions provided are in millimeters.

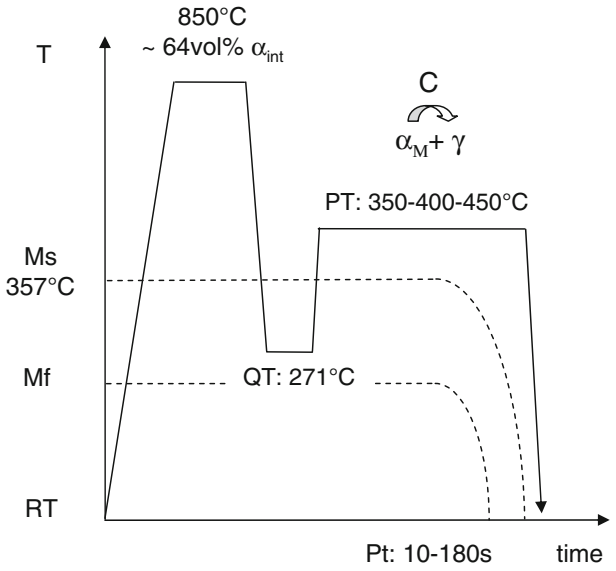

Fig. 2—Schematic representation of the applied heat treatments. After soaking at 850 °C, resulting in an intercritical microstructure containing 64 vol pct intercritical ferrite (α_{int}), the steel is quenched to 271 °C. After 3 s at that temperature, the samples are reheated to either 350 °C, 400 °C, or 450 °C and held for times ranging from 10 to 180 s, followed by a final water quench.

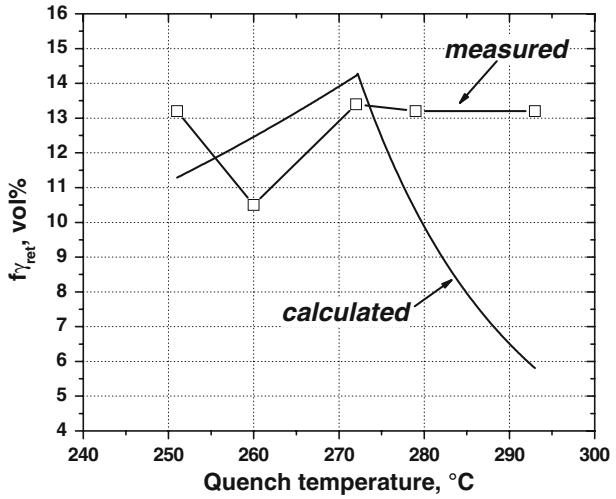

Fig. 3—Calculated and measured austenite volume fractions for varying QTs. Calculations were performed assuming full martensite depletion. The experimental values were obtained for 120 s of partitioning at 400 °C.

in agreement with Clarke *et al.*[13,21] A QT of 271 °C was chosen for subsequent heat treatments; the sample was held at this temperature for 3 seconds before beginning the partitioning treatment. Partitioning was performed at 350 °C, 400 °C, and 450 °C for times of 10, 60, 120, and 180 seconds.

Tensile testing was performed at a constant strain rate of $5.6 \cdot 10^{-4}$/s on an Instron* 5569 screw-driven tensile frame. The retained austenite volume fractions were measured *via* magnetic saturation (MS) measurements[22] and X-ray diffraction (XRD). The measurements were performed at room temperature and therefore incorporate the decrease in austenite upon final quenching where fresh martensite may form. Formation of fresh martensite during final quenching is especially likely at short partitioning times and low temperatures. An average of 4 MS measurements was used. In TRIP steels, retained austenite volume fractions obtained *via* MS have been shown to be a factor 1.4 greater than the volume fractions obtained *via* XRD.[23,24] X-ray analysis was also used to determine retained austenite volume fractions and carbon contents. A Siemens** D5000 diffractometer using Mo K_α radiation operating at 50 kV and 50 mA was used. Samples were scanned over a 2θ range from 15 to 55 deg, at a step size of 0.02 deg, with a dwell time of 1 second. The background radiation and $K_{\alpha 2}$ contributions to intensity were stripped. The retained austenite volume fraction was determined with the direct comparison method[25] using the integrated intensity of the $(200)_\alpha$, $(211)_\alpha$, $(220)_\gamma$, and $(311)_\gamma$ peaks. The carbon content was determined according to Cullity.[25] The average carbon content obtained from both austenite peak positions was calculated. Transmission electron microscopy (TEM) was carried out on a PHILIPS† CM120 operating at 120 kV. Thin specimens were electropolished with a Fischione‡ twin-jet polisher operating at 32 V at room temperature, using a mixture of 95 pct acetic acid and 5 pct perchloric acid.

*Instron is a trademark of Instron Corporation, Canton, MA.

**Siemens is a trademark of Siemens AG, Munich, Germany.

†PHILIPS is a trademark of Philips Electronics Instruments Corp., Mahwah, NJ.

‡Fischione is a trademark of E.A. Fischione Instruments Inc., Export, PA.

IV. MECHANICAL PROPERTIES OBTAINED *VIA* Q&P PROCESSING

The mechanical properties obtained *via* Q&P heat treating according to the scheme of Figure 2 are shown in Figure 4. Tensile strengths in the 770 to 1050 MPa range are obtained for this range of processing parameters (Figure 4(a)). The values decrease with increasing PT and time. The yield strengths vary from 440 to 590 MPa (Figure 4(a)). Unlike the tensile strengths, the yield strengths are not directly correlated with partitioning time or temperature. The volume fractions of retained austenite increase with increasing PT, as shown in Figure 4(c). A maximum volume fraction as function

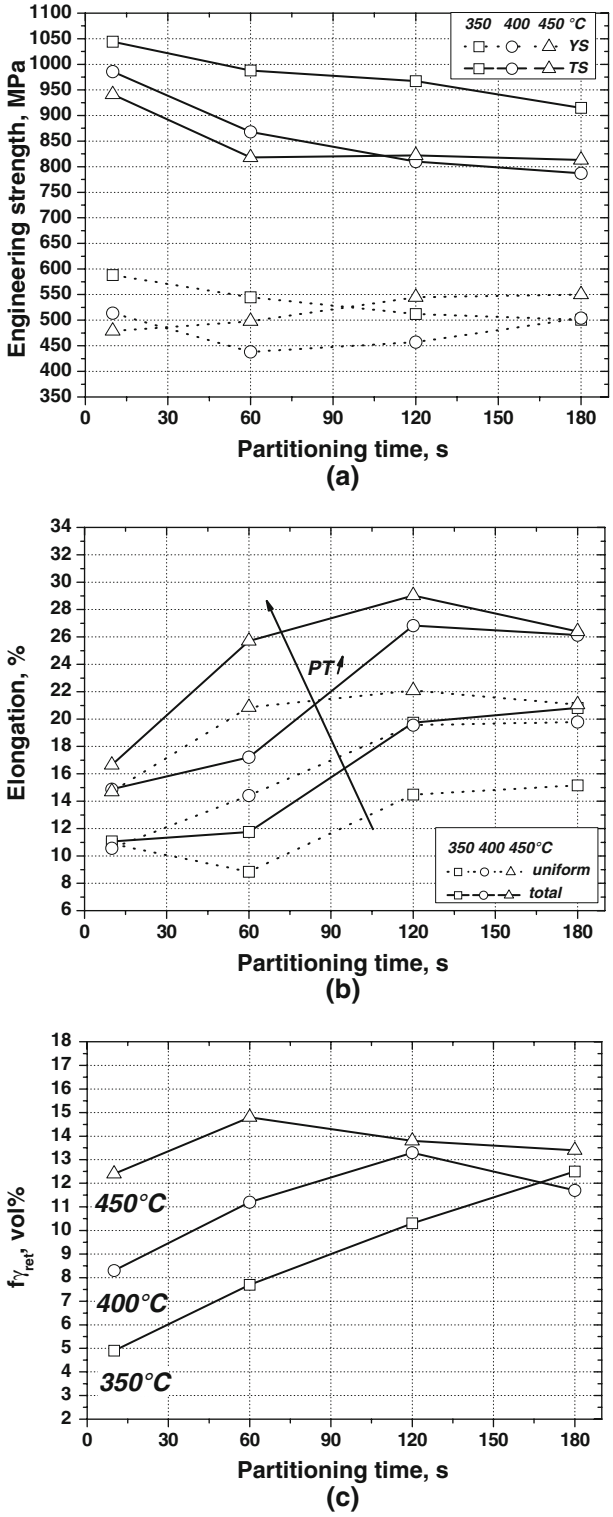

Fig. 4—Mechanical properties obtained for a CMnAlSiP steel *via* Q&P processing after intercritical annealing at 850 °C: (*a*) tensile and 0.2 pct offset yield strength, (*b*) uniform and total elongation, and (*c*) retained austenite volume fraction *vs* partitioning time as measured with MS for different PTs.

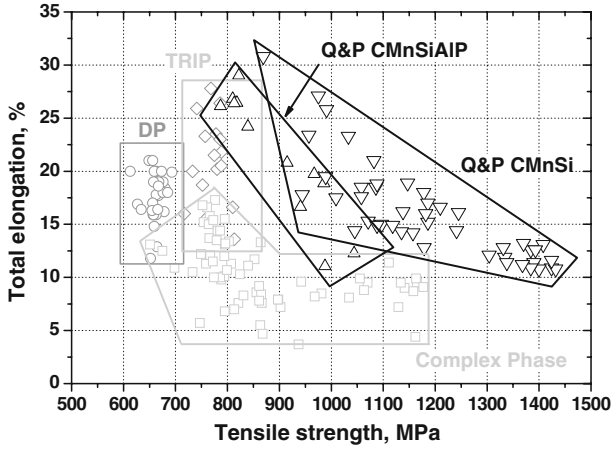

Fig. 5—Comparison of the mechanical properties obtained *via* Q&P processing and other recently developed high-strength steels.[26] The total elongation is plotted as function of tensile strength. Results obtained by Clarke *et al.*[13] *via* Q&P processing of a 0.19C-1.59Mn-1.63Si (wt pct) steel are also indicated in the graph.

of partitioning time is observed for partitioning at 400 °C and 450 °C in the timeframes examined. The decrease in retained austenite fraction at higher PTs and longer times is similar to the behavior of austempered TRIP steels, where cementite formation eventually occurs, leading to decomposition of retained austenite and formation of ferrite and iron carbide. Decomposition of the austenite by mechanisms other than cementite precipitation, such as bainite formation or γ/α_M interface movement, could also contribute to reduced amounts of austenite. In-depth studies to examine this behavior are needed, and do not appear to have been reported to date. The elongations increase with increasing partitioning time and temperature (Figure 4(b)). As shown in Figure 5, attractive combinations of strength and ductility are obtained. Tensile strengths of 800 MPa are combined with total elongations of at least 25 pct, whereas tensile strengths of 900 MPa are associated with about 20 pct total elongation. The highest tensile strength levels, 1000 to 1050 MPa, achieved by the processing performed here exhibit more than 10 pct total elongation. In this way, Q&P enables a broad spectrum of mechanical properties to be obtained with a single chemical composition by changing one process parameter, such as the PT. Properties obtained by Clarke *et al.*[13] for a 0.19C-1.59Mn-1.63Si (wt pct) composition for subsized tensile samples are also shown in Figure 5. Quench and partitioning was performed after intercritical annealing resulting in ~50 or ~25 vol pct of intercritical ferrite. PTs ranging from 350 °C to 450 °C and times ranging from 10 to 1000 seconds were used. Similar property levels are observed in the two studies with overlapping property envelopes, although the apparent property combinations are slightly better in the work of Clarke *et al.*, which employed subsized specimens. Figure 5 also provides a general comparison of the mechanical properties obtained *via* Q&P with those obtained on other "lean" compositions processed by other recently developed processing routes and microstructures, namely, DP, TRIP, and complex phase (CP).[26] The results in the figure show that Q&P provides properties that

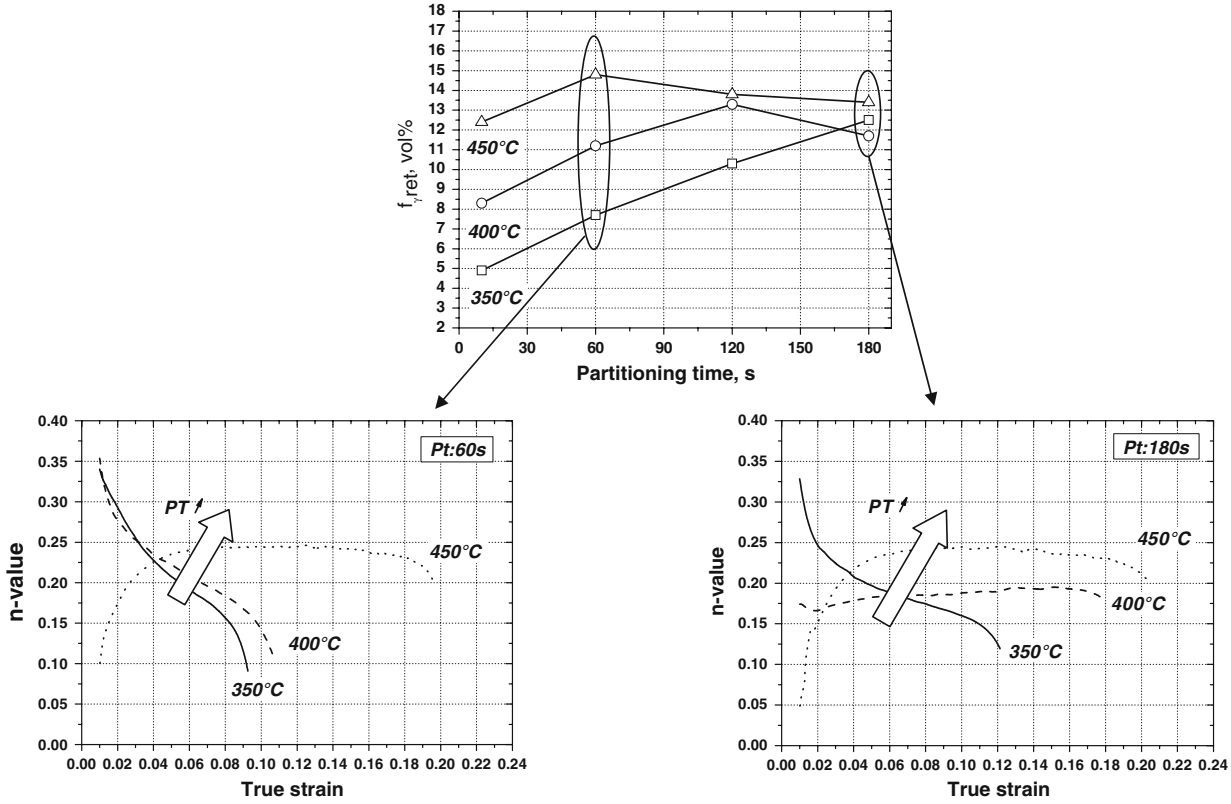

Fig. 6—Instantaneous strain hardening (*n*-value) for a partitioning time of 60 and 180 s for all PTs examined. A pronounced dependency of the strain hardening on the partitioning conditions is observed.

should be interesting relative to other processing options.

The instantaneous strain hardening (*n*-value) behavior as defined by

$$n = \frac{\partial \ln \sigma}{\partial \ln \varepsilon} = \frac{\ln \sigma_2 - \ln \sigma_1}{\ln \varepsilon_2 - \ln \varepsilon_1} \qquad [1]$$

with ε, true strain, and σ, true stress, is shown in Figure 6 *vs* true strain for partitioning times of 60 and 180 seconds for all three PTs examined. The strain hardening obtained after 60 seconds of partitioning exhibits a pronounced dependency on the PT applied. A PT of 350 °C or 400 °C results in a continuously decreasing *n*-value with strain, whereas at a higher PT of 450 °C, the *n*-value initially increases and maintains a high value for considerable amounts of strain. Note that the strain hardening obtained after partitioning at 350 °C or 400 °C is similar to the strain hardening obtained for DP steels,[27] whereas partitioning at 450 °C results in a TRIP steel type of strain hardening.[20] This type of strain hardening was also frequently exhibited after Q&P heat treatment following intercritical annealing of a high-Si grade for PTs of 350 °C, 400 °C, and 450 °C for times ranging from 10 to 1000 seconds.[13] In the current work, after 180 seconds of partitioning, comparable volume fractions of austenite are retained for each PT examined. Comparing the strain hardening curves obtained after partitioning for 60 seconds with those obtained after partitioning for 180 seconds, similar trends with strain are observed for 350 °C and 450 °C, but different strain hardening behaviors are exhibited for a PT of 400 °C. Partitioning for 180 seconds at that temperature results in strain hardening similar to austenite-containing TRIP steels, as mentioned previously. Oscillations in the instantaneous *n*-value curves occur at a given strain threshold: at 450 °C for 60 seconds and at 400 °C for 180 seconds, which are thought to be related to dynamic strain aging.[28]

A variety of different characteristics, such as austenite volume fraction and its carbon content, internal stresses (especially in the ferrite), carbide precipitation, dislocation density, *etc.* may alter when changing the partitioning conditions. These aspects will likely influence strain hardening. A comparison with austempered (TRIP) and Q&T microstructures may give further insight regarding the predominant mechanisms governing the strain hardening behavior of Q&P steels.

V. STRAIN HARDENING OF Q&P, TRIP, AND Q&T STEELS

The strain hardening after Q&P processing is compared with the strain hardening after Q&T and TRIP (*i.e.* austemper) processing in Figure 7 for the same steel and (aus)tempering or partitioning conditions (time and temperature). The corresponding mechanical properties

for the different microstructures are given in Table I. Figure 7(a) shows the engineering stress/strain curves and instantaneous *n*-values for Q&P and Q&T steels at a partitioning/tempering time of 180 seconds. Higher yield and tensile strengths are observed for the tempered DP (Q&T) steels compared to the Q&P steels. Higher internal stresses and dislocation densities might be expected in the tempered DP microstructures, because the initial quench was taken all the way to room temperature. In addition, the martensite fraction and the martensite carbon content may be higher in the Q&T steels. The Q&T steels show yield point elongations

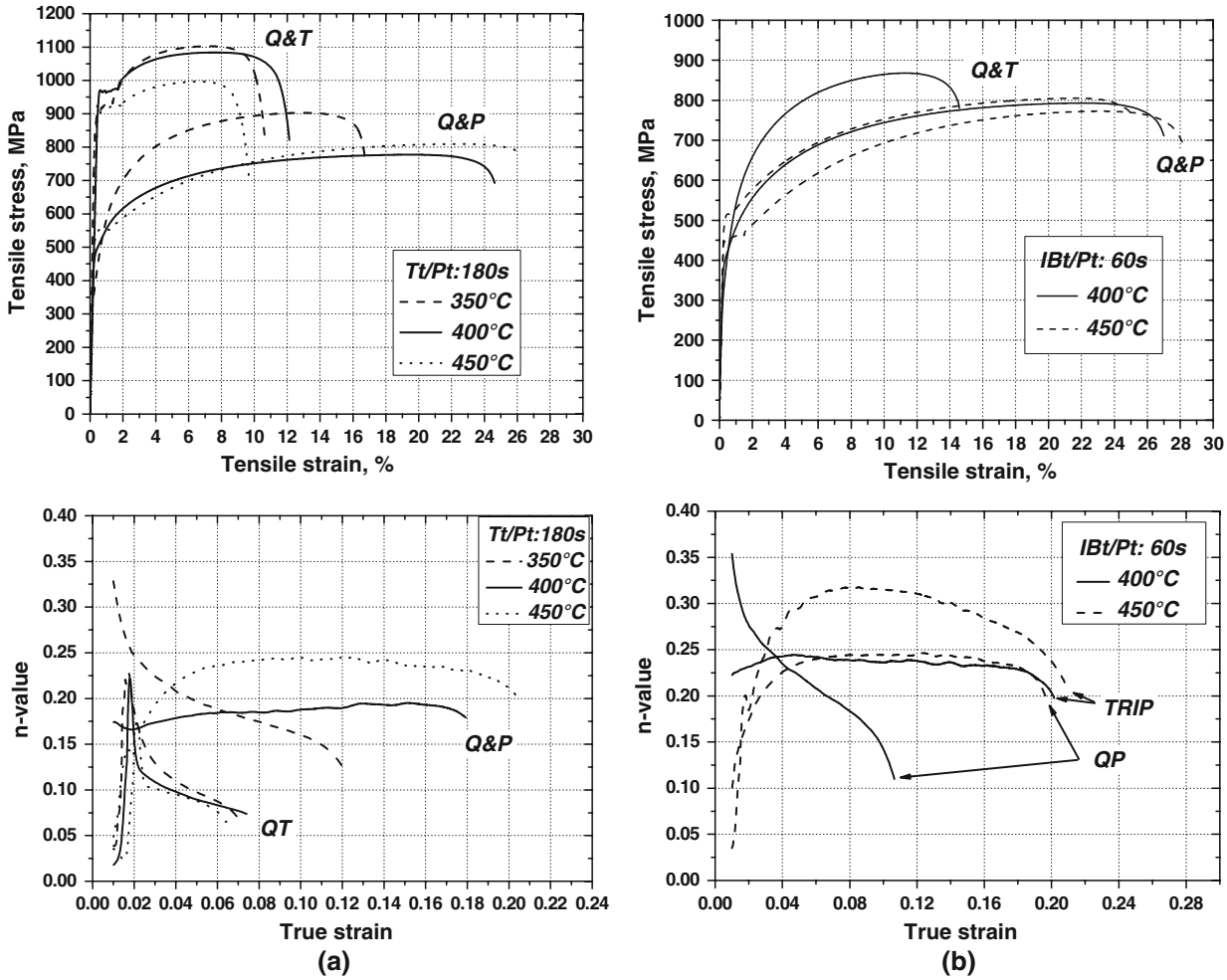

Fig. 7—Comparison of the engineering stress-strain curves and strain hardening of Q&P, Q&T, and TRIP steels.

Table I. Mechanical Properties Obtained for the Different Microstructures for Different Heat-Treatment Conditions; Austenite Volume Fractions Measured *via* MS and XRD and Austenite Carbon Contents are also Indicated

	PT/TT/IBT (°C)	Pt/Tt/IBt (s)	YS (MPa)	TS (MPa)	Au (Pct)	Atot (Pct)	$f\gamma_{ret}$ MS (Vol Pct)	$f\gamma_{ret}$ XRD (Vol Pct)	C Content (Wt Pct)
Q&P	350	180	420	903	12.5	16.8	12.5	6.4	0.97
	400	180	495	777	19.1	24.8	11.7	9.0	1.18
	450	180	549	809	21.8	27.3	13.4	10.0	1.10
	350	60	507	961	8.8	11.8	7.7	4.0	0.67
	400	60	438	868	14.4	17.2	11.2	4.5	0.96
	450	60	498	818	20.9	25.7	14.8	8.5	1.02
Q&T	350	180	910	1102	6.7	10.6	—	—	—
	400	180	967	1084	7.3	12.1	—	—	—
	450	180	904	995	5.9	9.7	—	—	—
TRIP	400	60	412	793	21.5	27.0	16.4	7.6	1.14
	450	60	451	772	22.6	28.2	16.0	10.0	1.04

(YPEs) for all tempering temperatures, whereas YPE is only observed when partitioning was done at 450 °C for the Q&P steels. Consistent with the reduced strength, the total elongations are significantly higher for the Q&P steels and increase with increasing PT. Note that the higher strength levels obtained after partitioning at a lower PT may be associated with carbon trapping or precipitation in the martensite. It is possible that more carbon depletion occurs at a higher PT, which may contribute to austenite retention but lower the strength of the martensite. Increasing the tempering temperature increases the elongation initially in the Q&T steels, although the elongation drops after tempering at 450 °C. The lower strength in combination with lower ductility after tempering at 450 °C may be associated with a mechanism similar to the well-known tempered martensite embrittlement phenomenon,[29] where retained austenite films decompose and are replaced by ferrite and more brittle cementite. No decrease in ductility with increased PT is observed for the same partitioning conditions, presumably because retained austenite is stabilized and not decomposed. The Q&T steels exhibit much less strain hardening, consistent with their higher strength. Continuously decreasing instantaneous *n*-value curves are also observed for all tempering temperatures, whereas only at a PT of 350 °C was this the case for the Q&P steels.

Figure 7(b) shows the tensile graphs and the strain hardening for austempered (TRIP) and Q&P heat treated samples. Austempering/partitioning involved 60 seconds at 400 °C to 450 °C. Because the M_s temperature of the austenite present at the intercritical annealing temperature was 357 °C as measured *via* dilatometry, there was no isothermal bainitic treatment (IBT, *i.e.* austempering) done at 350 °C. Comparable amounts of retained austenite are obtained for partitioning at 450 °C and austempering at 400 °C (Table I).

The highest strength level is obtained for the Q&P steel partitioned at 400 °C. Continuously decreasing instantaneous *n*-value with strain is associated with this condition. Partitioning at 450 °C leads to very similar strain hardening and stress/strain curves as austempering at 400 °C. The similar mechanical behavior of the Q&P and TRIP steels for these two conditions suggests that the mechanical stability of the retained austenite is similar. Austempering at 450 °C leads to lower strength levels with greater elongation and strain hardening.

VI. ANALYSIS USING AUSTENITE STABILITY MODELS

As discussed previously, significantly greater strain hardening is observed for Q&P steels compared to Q&T steels with similar partitioning/tempering treatments. Much lower amounts of retained austenite, but higher internal stresses and dislocation densities, are expected to be present in the latter. Similar strain hardening characteristics are observed for Q&P and austempered microstructures containing similar volume fractions of retained austenite. Austempered TRIP microstructures are known to have increased strain hardening and delayed necking due to the strain-induced martensitic transformation of the metastable retained austenite.[30] The rate of this transformation upon straining is an important parameter in this regard.

The mechanical stability of the retained austenite in TRIP and Q&P steels measured by MS after interrupted tensile testing is shown in Figure 8. Several models have been proposed to describe the stability of austenitic stainless steels.[31–33] These models have been successfully applied to multiphase materials such as low-carbon TRIP steels.[30] The Ludwigson–Berger and Olson–Cohen models will be considered in the present contribution; their relationships are given in Eqs. [2] and [3], respectively.

$$\frac{1}{V_\gamma} - \frac{1}{V_{\gamma_0}} = \frac{k_p}{p}\varepsilon^p \qquad [2]$$

$$f_{\alpha'} = 1 - \exp\left[-\beta[1 - \exp(-\alpha\varepsilon)]^2\right] \qquad [3]$$

with V_γ the austenite fraction at a true strain ε, V_{γ_0} the initial austenite fraction in the unstrained material, p the autocatalytic factor, $f_{\alpha'}$ the volume fraction of austenite transformed to martensite, k_p, α, and β constants related to the austenite stability. The parameters obtained after fitting the data of Figure 8 with the described models are given in Table II.

In general, lower k_p and p values are obtained for the Q&P steels, suggesting higher austenite stability and less autocatalytic propagation in the context of the Ludwigson–Berger model. Autocatalytic propagation is the phenomenon whereby the formation of martensite promotes the nucleation of more, fresh martensite. If the strain-induced martensite encounters a second phase, such as intercritical ferrite or bainite laths for TRIP steels, the autocatalytic effect is reduced.[32] Hence, an increase in second phase volume fraction and a finer distribution of the latter leads to a decrease of the autocatalytic effect and decreasing p values. In

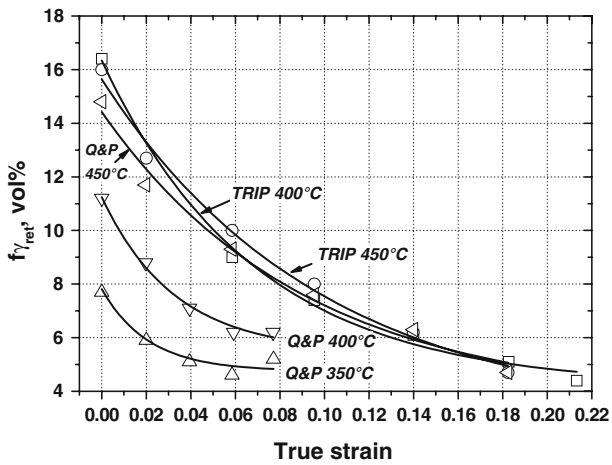

Fig. 8—Mechanical stability of the retained austenite present in austempered and Q&P microstructures measured after interrupted tensile testing. Measurements were done using MS. Austempering/partitioning time was 60 s.

Table II. Parameters Obtained after Fitting the Data in Figure 6 with the Models of (a) Ludwigson–Berger and (b) Olson–Cohen

(a)

	kp		p	
IBT/PT	TRIP	Q&P	TRIP	Q&P
350 °C	—	16 ± 7	—	0.52 ± 0.10
400 °C	71 ± 6	33 ± 6	0.97 ± 0.02	0.71 ± 0.03
450 °C	158 ± 9	120 ± 13	1.26 ± 0.12	1.17 ± 0.12

(b)

	α		β	
IBT/PT	TRIP	Q&P	TRIP	Q&P
350 °C	—	71 ± 6	—	0.46 ± 0.09
400 °C	19 ± 3	52 ± 7	1.25 ± 0.10	0.63 ± 0.04
450 °C	18 ± 10	21 ± 12	1.15 ± 0.16	1.02 ± 0.18

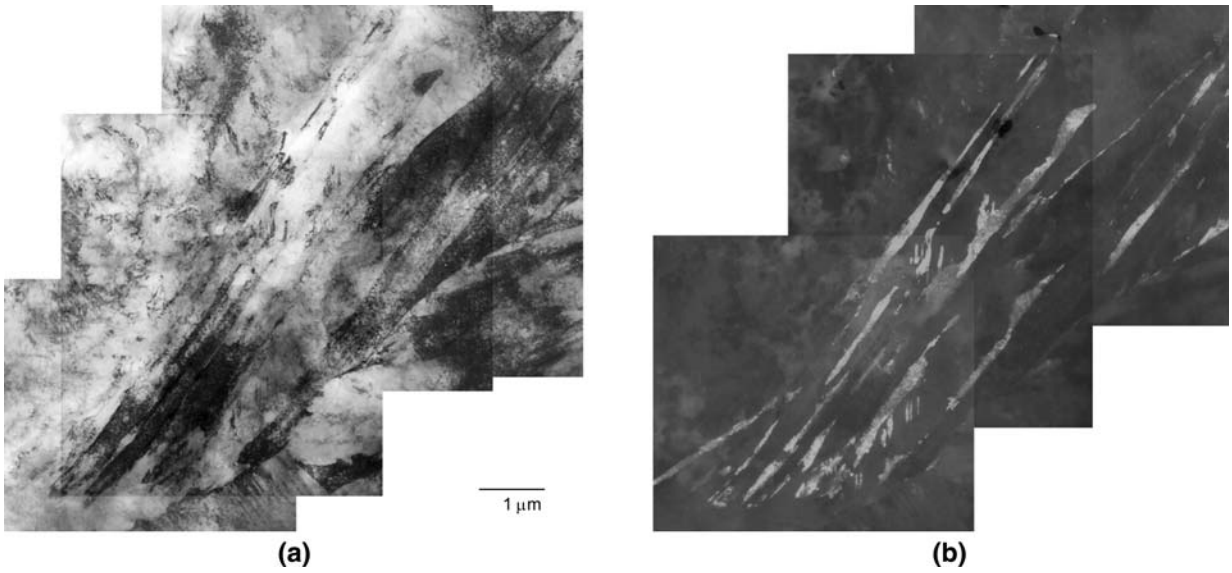

Fig. 9—TEM micrograph of a Q&P microstructure: (*a*) bright-field image and (*b*) dark-field image taken with an austenite reflection. Microstructure consists of fine martensitic laths with a high dislocation density. Austenite has a filmlike appearance, separating the martensite laths.

this way, duplex stainless steels have $p = 2$, whereas $p = 3$ is obtained for austenitic stainless steels.[32] The value $p = 1$ has been reported for austempered microstructures, in good agreement with the present experimental data for TRIP microstructures.[30,32,34]

A TEM micrograph of a Q&P microstructure (PT: 400 °C) is given in Figure 9(a). A dark-field image of the retained austenite is given in Figure 9(b). The microstructure consists of fine martensitic laths with high dislocation density. The retained austenite is present as laths or fine films separating the martensite laths. The scale and morphology of the γ appears different in Q&P steels compared to TRIP microstructures. In austempered TRIP microstructures, the austenite is reported to be present as large blocky grains and thicker laths.[30] These differences may result in a smaller autocatalytic effect and, hence, lower p values for Q&P steels.

A smaller grain size is known to increase austenite stability due to effects related to the population of potential nuclei. Krizan[35] reports a k_p value of 55 for a Ti microalloyed CMnSiAlP TRIP steel with an average retained austenite grain size of 800 nm and a carbon content of 1.10 wt pct. A higher value of $k = 132$ was obtained for a CMnSiAlP TRIP steel where no microalloying elements were added. A coarser retained austenite grain size of 1.4 μm was measured in this case with an austenite carbon content of 1.13 wt pct. Higher k_p values are obtained for the TRIP microstructures compared to the Q&P microstructures, which may also be related to the finer scale of the austenite retained by Q&P (Table II). An increase in PT leads to increasing k_p values for the Q&P steels here. Table I indicates that a higher carbon content is obtained after partitioning at 400 °C as compared to partitioning at 350 °C, which

may imply chemical stabilization of the austenite against transformation. Relaxation of internal stresses at higher PTs may influence the transformation behavior, although it should be noted that the overall austenite fractions are higher and austenite composition gradients may also be reduced.

Higher α and lower β parameter values are obtained for the Q&P steels after fitting with the Olson–Cohen model for strain-induced transformation. This model considers nucleation of martensite embryos on the intersections of shear bands, such as dense stacking faults, twins, and ε martensite.[33] The α is a measure for the nucleation rate of these shear bands and is related to the stacking fault energy (SFE), increasing with decreasing SFE. Higher α values result in easier nucleation. The β is a measure for the driving force available for the martensite transformation to take place. It is related to the Gibbs free energy difference $\Delta G^{\gamma\rightarrow\alpha'}$. More driving force results in higher β values. The onset temperature M_s^σ for strain-induced transformation can help characterize retained austenite stability. The M_s^σ temperature measurement for the Q&P steel partitioned at 350 °C using the method proposed by Haedemenopoulos *et al.*[36] is given in Figure 10. Deformation temperature dependent yielding behavior is observed. Strain-induced transformation is associated with continuous yielding; the austenite first yields and stacking faults are generated. The intersections of these stacking faults serve as effective nucleation sites for martensite embryos. Stress-assisted martensite nucleates on pre-existing sites and is associated with discontinuous yielding. The M_s^σ temperature separates both transformation regimes. An M_s^σ temperature of 10 °C is obtained, meaning that deformation at room temperature results in strain-induced transformation. Thus, the Olson–Cohen model may be applied for Q&P steels. Similar M_s^σ temperatures are reported for TRIP steels having similar austenite compositions.[37] Note that the absence of YPE for the Q&P steels compared to the Q&T steels (Figure 7) may be

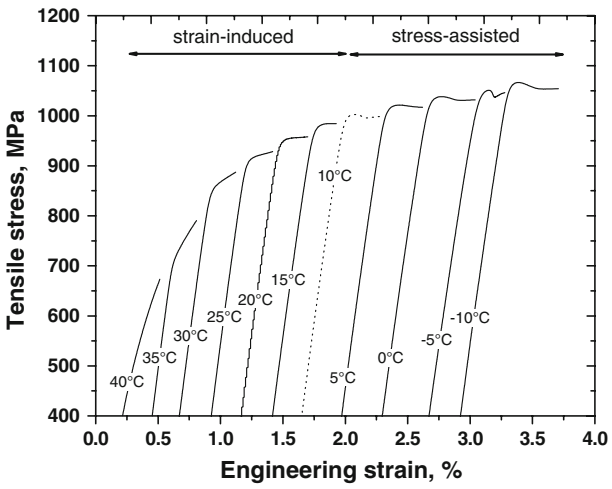

Fig. 10—M_s^σ temperature measurement for the Q&P steel partitioned at 350 °C. Transition from strain-induced to stress-assisted transformation occurs when the testing temperature is decreased and is associated with the occurrence of a yield drop. An M_s^σ temperature of 10 °C is obtained.

associated with strain-induced transformation of the austenite. The yielding of the complex Q&P aggregate is governed by the yielding of the retained austenite. The Q&T steels contain much less retained austenite, so yielding is governed by dislocation motion.

The α and β values obtained suggest that less driving force (lower β values) may be available for the transformation to take place in Q&P steels compared to TRIP microstructures, although the formation of stacking faults (higher α values) may be easier in Q&P steels. These differences are more pronounced at lower partitioning/austempering temperatures. Partitioning/austempering at 450 °C leads to similar α and β values for both microstructures. Note also that similar carbon contents are obtained for this temperature.

The Q&P steel partitioned at 350 °C results in the highest α value and lowest β value. The lowest carbon content was measured for this steel, resulting in lower SFE, which facilitates stacking fault formation and results in a higher α value. The lower β value suggests a lower driving force for the transformation to take place. This is in contrast with the expected effect of a lower austenite carbon content, which implies a higher driving force and lower stability. The lower β value may be related to internal compressive stresses opposing the austenite transformation. These stresses are introduced during the initial quenching due to the volume expansion associated with the martensite formation and are relaxed during subsequent partitioning. The lower the quenching and PTs applied, the greater the internal stresses.

It should be noted that, although the austenite stability models have been applied successfully for multiphase materials,[30] they were originally developed for fully austenitic stainless steels. Applying the models to multiphase materials by using the macroscopic true strain in Eqs. [2] and [3] does not take into account strain partitioning between the different constituents. Large hardness differences between the phases will influence the strain partitioning, and hence may influence the values obtained for the parameters.

VII. CONCLUSIONS

Quench and partitioning is shown to be an effective way to produce high strength steels with good ductility containing stabilized retained austenite in a martensitic microstructure. Tensile strength/total elongation combinations range for a given steel, intercritical treatment, and QT, depending on the partitioning conditions, from 800 MPa/>25 pct to 900 MPa/20 pct and 1000 MPa/10 pct, suggesting great flexibility for Q&P product applications. The strain hardening exhibited by Q&P steels shows significant dependence on PT and time, and is intermediate between the strain hardening behavior of Q&T (tempered DP) and austempered steels for the same (aus)tempering/partitioning conditions applied. The measured mechanical stability of the retained austenite indicates that the TRIP effect occurs in Q&P steels, thereby effectively contributing to its strain hardening.

ACKNOWLEDGMENTS

The Institute for the Promotion of Innovation through Science and Technology in Flanders (IWT–Vlaanderen) is gratefully acknowledged for funding this research. The support of Arcelor-Mittal Research Industry Ghent (OCAS) and the sponsors of the Advanced Steel Processing and Products Research Center (ASPPRC), an industry/university cooperative research center at the Colorado School of Mines, is also gratefully acknowledged. Special thanks go to Gary Zito, Bob McGrew, and Professor S.W. Thompson for their support in TEM sample preparation and analysis.

REFERENCES

1. J.G. Speer, D.K. Matlock, B.C. De Cooman, and J.G. Schroth: *Acta Mater.*, 2003, vol. 51, pp. 2611–22.
2. W.S. Owen: *Trans. ASM*, 1954, vol. 46, pp. 812–29.
3. W.S Owen: *J. Iron Steel Inst.*, 1951, vol. 167, pp. 117–20.
4. S.J. Bernard, G.D.W. Smith, A.J. Garratt-Reed, and J. Vander Sande: in *Solid-Solid Phase Transformations*, H.I. Aaronson, D.E. Laughlin, R.F. Sekerka, and C.M. Wayman, eds., TMS-AIME, Warrendale, PA, 1981, pp. 881–85.
5. J. Mahieu, S. Claessens, and B.C. De Cooman: *Metall. Trans. A*, 2001, vol. 32A, pp. 2905–08.
6. J. Mahieu, J. Maki, B.C. De Cooman, M. Fiorucci, and S. Claessens: *Mater. Sci. Technol.*, 2003, vol. 19, pp. 125–31.
7. G.R. Speich and W.C. Leslie: *Metall. Trans.*, 1972, vol. 3, pp. 1043–54.
8. G.R. Speich and K.A. Taylor: in *Martensite*, G.B. Olson and W.S. Owen, eds., ASM International, Materials Park, OH, 1992, pp. 243–75.
9. G. Krauss: in *Proc. Int. Conf. on Phase Transformations in Ferrous Alloys*, A.R. Marder and J. I. Goldstein, eds., TMS-AIME, Warrendale, PA, 1984, pp. 101–23.
10. A.J. Shutts, J.G. Speer, D.K. Matlock, D.V. Edmonds, F. Rizzo, and E.B. Damm: in *Proc. Int. Conf. on New Developments in Long and Forged Products: Metallurgy and Applications*, J.G. Speer, E.B. Damm, and C.V. Darragh, eds., AIST, 2006, pp. 191–202.
11. J. Wong, D.K. Matlock, and G. Krauss: *Proc. 43rd MWSP Conf.*, ISWS, Warrendale, PA, 2001, vol. 39, pp. 21–36.
12. D.V. Edmonds, K. He, M.K. Miller, F.C. Rizzo, A. Clarke, D.K. Matlock, and J.G. Speer: *Mater. Sci. Forum*, 2007, vols. 539–543, pp. 4819–25.
13. A.J. Clarke: Ph.D. Thesis, Colorado School of Mines, Golden, CO, 2006.
14. E. De Moor, S. Lacroix, L. Samek, J. Penning, and J.G. Speer: *Proc. 3rd ICASS*, Geongju, Korea, 2006, pp. 873–78.
15. E. De Moor: Ghent University, unpublished research, 2007.
16. N. Zhong, X. Wang, Y. Rong, and L. Wang: *J. Mater. Sci. Technol.*, 2006, vol. 22 (6), pp. 751–54.
17. J.G. Speer, R.E. Hackenberg, B.C. De Cooman, and D.K. Matlock: *Philos. Mag. Lett.*, 2007, vol. 87 (6), pp. 379–82(4).
18. A.J. Clarke, J.G. Speer, M.K. Miller, R.E. Hackenberg, D.V. Edmonds, D.K. Matlock, F.C. Rizzo, K.D. Clarke, and E. De Moor: *Acta Mater.*, 2008, vol. 56 (1), pp. 16–22.
19. B.C. De Cooman and J.G. Speer: *Steel Res. Int.*, 2006, vol. 77 (9–10), pp. 634–40.
20. J. Mahieu, J. Maki, B.C. De Cooman, and S. Claessens: *Metall. Mater. Trans. A*, 2002, vol. 33A, pp. 2573–80.
21. A. Clarke, J.G. Speer, D.K. Matlock, F.C. Rizzo, D.V. Edmonds, and K. He: in *Solid-Solid Phase Transformations in Inorganic Materials 2005*, J.M. Howe, D.E. Laughlin, U. Dahmen, J.K. Lee, and D.J. Srolovitz, eds., TMS, Warrendale, PA, 2005, vol. 2, pp. 99–108.
22. L. Zhao, N.H. Van Dijk, E. Brück, J. Sietsma, and S. van der Zwaag: *Mater. Sci. Eng. A*, 2001, vol. A313, pp. 145–52.
23. D. Krizan, J. Antonissen, and B.C. De Cooman: in *Proc. Int. Conf. on Advanced High Strength Sheet Steels for Automotive Applications*, M.A. Baker and R.E. Ashburn, eds., AIST, Winter Park, 2004, pp. 205–16.
24. M. De Meyer, D. Vanderscheuren, K. De Blauwe, and B.C. De Cooman: *Proc. 41st MWSP Conf.*, ISS, Baltimore, MD, 1999, vol. XXXVII, pp. 483–91.
25. B.D. Cullity and S.R. Stock: *Elements of X-ray Diffraction*, 3rd ed., Prentice Hall, New York, 2001, pp. 215–42.
26. C. Mesplont, S. Vandeputte, and B.C. De Cooman: *Proc. 43rd MWSP Conf.*, ISS, Warrendale, PA, 2001, vol. 39, pp. 359–71.
27. O. Yakubovsky, N. Fonstein, and D. Bhattacharya: in *Proc. Int. Conf. on Advanced High-Strength Sheet Steels for Automotive Applications*, J.G. Speer, ed., AIST, Warrendale, PA, 2004, pp. 295–06.
28. S. Okamoto, D.K. Matlock, and G. Krauss: *Scripta Metall.*, 1991, vol. 25A, pp. 39–44.
29. M. Sarikaya, A.K. Jhingan, and G. Thomas: *Metall. Trans. A*, 1983, vol. 14A, pp. 1121–33.
30. L. Samek, E. De Moor, J. Penning, and B.C. De Cooman: *Metall. Mater. Trans. A*, 2006, vol. 37A, pp. 109–24.
31. T. Angel: *J. Iron Steel Inst.*, 1954, vol. 177, pp. 165–74.
32. D.C. Ludwigson and J.A. Berger: *J. Iron Steel Inst.*, 1969, vol. 207, pp. 63–69.
33. G.B. Olson and M. Cohen: *Metall. Trans. A*, 1975, vol. 6A, pp. 791–95.
34. O. Matsumura, Y. Sakuma, and H. Takechi: *Scripta Metall.*, 1987, vol. 21, pp. 1301–06.
35. D. Krizan: Ph.D. Thesis, Ghent University, Ghent, Belgium, 2005.
36. G.N. Haidemenopoulos, M. Grujicic, G.B. Olson, and M. Cohen: *Acta Metall.*, 1989, vol. 37 (6), pp. 1677–82.
37. L. Barbé, M. De Meyer, and B.C. De Cooman: in *Proc. Int. Conf. on TRIP-Aided High Strength Ferrous Alloys*, B.C. De Cooman, ed., Ghent, Belgium, 2002, pp. 65–69.